



Measurement of the branching ratio and search for a CP violating asymmetry in the $\eta \rightarrow \pi^+ \pi^- e^+ e^- (\gamma)$ decay at KLOE

KLOE Collaboration

F. Ambrosino^{c,d}, A. Antonelli^a, M. Antonelli^a, F. Archilli^{h,i}, P. Beltrame^b, G. Bencivenni^a, S. Bertolucci^a, C. Bini^{f,g}, C. Bloise^a, S. Bocchetta^{j,k}, F. Bossi^a, P. Branchini^k, G. Capon^a, T. Capussela^a, F. Ceradini^{j,k}, P. Ciambro^a, F. Crucianelli^f, E. De Lucia^a, A. De Santis^{f,g}, P. De Simone^a, G. De Zorzi^{f,g}, A. Denig^b, A. Di Domenico^{f,g}, C. Di Donato^d, B. Di Micco^{j,k}, M. Dreucci^a, G. Felici^a, S. Fiore^{f,g}, P. Franzini^{f,g}, C. Gatti^a, P. Gauzzi^{f,g}, S. Giovannella^{a,*}, E. Graziani^k, G. Lanfranchi^a, J. Lee-Franzini^{a,1}, D. Leone^b, M. Martini^{a,e}, P. Massarotti^{c,d}, S. Meola^{c,d}, S. Miscetti^a, M. Moulson^a, S. Müller^a, F. Murtas^a, M. Napolitano^{c,d}, F. Nguyen^{j,k}, M. Palutan^a, E. Pasqualucci^g, A. Passeri^k, V. Patera^{a,e}, F. Perfetto^{c,d}, P. Santangelo^a, B. Sciascia^a, T. Spadaro^a, M. Testa^{f,g}, L. Tortora^k, P. Valente^g, G. Venanzoni^a, R. Versaci^{a,e,*}, G. Xu^{a,m}

^a Laboratori Nazionali di Frascati dell'INFN, Frascati, Italy

^b Institut für Kernphysik, Johannes Gutenberg-Universität Mainz, Germany

^c Dipartimento di Scienze Fisiche dell'Università "Federico II", Napoli, Italy

^d INFN Sezione di Napoli, Napoli, Italy

^e Dipartimento di Energetica dell'Università "La Sapienza", Roma, Italy

^f Dipartimento di Fisica dell'Università "La Sapienza", Roma, Italy

^g INFN Sezione di Roma, Roma, Italy

^h Dipartimento di Fisica dell'Università "Tor Vergata", Roma, Italy

ⁱ INFN Sezione di Roma Tor Vergata, Roma, Italy

^j Dipartimento di Fisica dell'Università "Roma Tre", Roma, Italy

^k INFN Sezione di Roma Tre, Roma, Italy

¹ Physics Department, State University of New York at Stony Brook, USA

^m Institute of High Energy Physics of Academica Sinica, Beijing, China

ARTICLE INFO

Article history:

Received 28 December 2008

Received in revised form 16 March 2009

Accepted 3 April 2009

Available online 10 April 2009

Editor: M. Doser

PACS:

13.66.Bc

14.40.Aq

11.30.Er

Keywords:

e^+e^- collisions

Rare η decays

CP violation

ABSTRACT

We have studied the $\eta \rightarrow \pi^+ \pi^- e^+ e^- (\gamma)$ decay using about 1.7 fb^{-1} collected by the KLOE experiment at the DAΦNE ϕ -factory. This corresponds to about 72 millions η mesons produced in ϕ radiative decays. We have measured the branching ratio, inclusive of radiative effects, with 4% accuracy: $BR(\eta \rightarrow \pi^+ \pi^- e^+ e^- (\gamma)) = (26.8 \pm 0.9_{\text{Stat.}} \pm 0.7_{\text{Syst.}}) \times 10^{-5}$. We have obtained the first measurement of the CP-odd $\pi\pi-ee$ decay planes angular asymmetry, $\mathcal{A}_\phi = (-0.6 \pm 2.5_{\text{Stat.}} \pm 1.8_{\text{Syst.}}) \times 10^{-2}$.

© 2009 Elsevier B.V. All rights reserved.

1. Introduction

The decay of light pseudoscalar mesons, π^0 , η and η' , proceeds via electromagnetic interaction and the radiative decays of η and η' to pions allow to probe their electromagnetic structure [1]. Conversion decays offer the possibility to measure precisely the virtual

* Corresponding authors at: Laboratori Nazionali di Frascati dell'INFN, Frascati, Italy.

E-mail addresses: simona.giovannella@lnf.infn.it (S. Giovannella), roberto.versaci@lnf.infn.it (R. Versaci).

photon 4-momentum via the invariant mass of the e^+e^- pair. The branching ratio for internal conversion decay of the η meson, $\eta \rightarrow \pi^+\pi^-e^+e^-$, has been computed with different approaches, but until recently both the theoretical and the experimental results were affected by large uncertainties.

The first calculation, based on pure QED, is 40 years old: $BR \sim 3 \times 10^{-4}$ [2]. The addition of $\pi\pi$ interaction treated with the Vector Dominance Model gives $BR = 3.6 \times 10^{-4}$ with an error of about 10% [3], while an approach based on chiral perturbation theory that includes vector mesons gives $(3.2 \pm 0.3) \times 10^{-4}$ [4]. Recently, an approach based on the chiral effective Lagrangian including $\pi\pi$ interactions has obtained a more precise result: $BR = (2.99^{+0.06}_{-0.09}) \times 10^{-4}$ [5].

The $\eta \rightarrow \pi^+\pi^-e^+e^-$ decay has been first observed by the CMD-2 experiment [6], giving $BR = (3.7^{+2.5}_{-1.8} \pm 3.0) \times 10^{-4}$, and has afterwards been confirmed by the CELSIUS-WASA experiment [7,8]: $BR = (4.3^{+2.0}_{-1.6} \pm 0.4) \times 10^{-4}$. The precision of these results does not allow to test different models.

Recently, a possible CP violating mechanism (CPV), not directly related to the most widely studied flavor changing neutral processes, has been proposed. This mechanism could induce interference between electric and magnetic decay amplitudes. Such CPV effect could be tested in the decays of the pseudoscalar mesons by measuring the polarization of the virtual photon and would result in an asymmetry in the angle ϕ between the planes containing the e^+e^- and the $\pi^+\pi^-$ pairs in the meson rest frame, defined as

$$\mathcal{A}_\phi = \frac{\int_0^{\pi/2} \frac{d\Gamma}{d\phi} d\phi - \int_{\pi/2}^{\pi} \frac{d\Gamma}{d\phi} d\phi}{\int_0^{\pi/2} \frac{d\Gamma}{d\phi} d\phi + \int_{\pi/2}^{\pi} \frac{d\Gamma}{d\phi} d\phi}.$$

This kind of asymmetry has been already studied [9–13] and observed [14,15] in the decay of the K_L meson. In the η decay this asymmetry is constrained, by experimental [16] and Standard Model [17] upper limits on the CP-violating decay $\eta \rightarrow \pi^+\pi^-$, to be, at most of $\mathcal{O}(10^{-4})$ and $\mathcal{O}(10^{-15})$, respectively. However, as pointed out in [18,19], it is possible in case of sources of CPV beyond the Standard Model which do not contribute directly either to ϵ_K or to the neutron electric dipole moment, d_n . In this case, \mathcal{A}_ϕ is predicted to be up to $\mathcal{O}(10^{-2})$, a value reachable with the present statistics of η mesons.

2. The KLOE detector

The KLOE experiment operates at DAΦNE, the Frascati ϕ -factory. DAΦNE is an e^+e^- collider running at a center of mass energy of ~ 1020 MeV, the mass of the ϕ meson. Equal energy positron and electron beams collide at an angle of $\pi - 25$ mrad, producing ϕ mesons nearly at rest.

The detector consists of a large cylindrical Drift Chamber, surrounded by a lead-scintillating fiber ElectroMagnetic Calorimeter (EMC). A superconducting coil around the EMC provides a 0.52 T field. The drift chamber [20], 4 m in diameter and 3.3 m long, has 12582 all-stereo tungsten sense wires and 37746 aluminum field wires. The chamber shell is made of carbon fiber-epoxy composite and the gas used is a 90% helium, 10% isobutane mixture. The position resolutions are $\sigma_{xy} \sim 150$ μm and $\sigma_z \sim 2$ mm. The momentum resolution is $\sigma(p_\perp)/p_\perp \approx 0.4\%$. Vertices are reconstructed with a spatial resolution of ~ 3 mm. The calorimeter [21] is divided into a barrel and two endcaps, for a total of 88 modules, and covers 98% of the solid angle. The modules are read out at both ends by photo-multipliers, both in amplitude and time. The readout granularity is $\sim (4.4 \times 4.4)$ cm^2 , for a total of 2440 cells arranged in five layers. The energy deposits are obtained from the signal amplitude while the arrival times and the particles positions are obtained from the time differences. Cells close in time and space are grouped into calorimeter clusters. The cluster energy E is the sum of the cell

energies. The cluster time T and position \vec{R} are energy-weighted averages. Energy and time resolutions are $\sigma_E/E = 5.7\%/\sqrt{E}$ (GeV) and $\sigma_t = 57$ ps/ \sqrt{E} (GeV) \oplus 100 ps, respectively. The trigger [22] uses both calorimeter and chamber information. In this analysis the events are selected by the calorimeter trigger, requiring two energy deposits with $E > 50$ MeV for the barrel and $E > 150$ MeV for the endcaps. A cosmic veto rejects events with at least two energy deposits above 30 MeV in the outermost calorimeter layer. Data are then analyzed by an event classification filter [23], which streams various categories of events in different output files.

3. Event selection

This analysis has been performed using 1733 pb^{-1} from the 2004–2005 dataset, 242 pb^{-1} from the 2006 off-peak ($\sqrt{s} = 1000$ MeV) data, 3447 pb^{-1} of Monte Carlo (MC) simulating all ϕ decays, 50506 pb^{-1} of signal Monte Carlo. Signal MC has been generated according to the matrix element in [19], with $BR = 4 \times 10^{-4}$ and having $\mathcal{A}_\phi = 0$. All MC productions account for run by run variation of the main data-taking parameters such as background conditions, detector response and beams configuration. Data-MC corrections for calorimeter clusters and tracking efficiency, evaluated with radiative Bhabha events and $\phi \rightarrow \rho\pi$ samples respectively, have been applied. Effects of Final State Radiation (FSR) have been taken into account using the PHOTOS MC package [24,25]. This package simulates the emission of FSR photons by any of the decay products taking also into account possible interference between different diagrams. We have inserted PHOTOS in our Monte Carlo at the event generation level, simulating FSR for the electrons, therefore our simulation fully accounts for radiative decays.

At KLOE, η mesons are produced together with a monochromatic recoil photon through the radiative decay $\phi \rightarrow \eta\gamma$ ($E_\gamma = 363$ MeV). In the considered data sample about 72×10^6 η 's are present. As first step of the analysis, a preselection is performed requiring at least four tracks (two positive and two negative) coming from the Interaction Point. The Fiducial Volume is defined by a cylinder having radius $R = 4$ cm and height $h = 20$ cm. For each charge, the two tracks with the highest momenta are selected. After track selection, one and only one neutral cluster, having energy $E_{\text{cl}} \geq 250$ MeV and polar angle in the range (23° – 157°), is required. A cluster is defined neutral if it does not have any associated track and has a time compatible with the photon time of flight. After preselection, the signal is about 1.4% of the sample.

Mass assignment for each track is performed by either identifying a pion decay from a kink in the track, or using the Time Of Flight (TOF) of the particles. For each track associated to a calorimeter cluster, the quantity $\Delta t = t_{\text{track}} - t_{\text{cluster}}$ in both electron (Δt_e) and pion (Δt_π) hypothesis is evaluated; t_{track} is defined as the length of the track divided by $\beta(m)c$. The mass hypothesis minimizing Δt is then chosen. If two tracks of the same charge satisfy the same mass hypothesis, the minimum Δt_e identifies the electron. When only one of the same charge tracks is identified as pion (electron), the other one is assumed to be electron (pion). For the remaining events the tracks with higher momentum are assumed to be pion.

To improve the energy and momentum resolution, a kinematic fit is performed imposing the four-momentum conservation and the TOF of the photon. A very loose cut on the χ^2 of the kinematic fit is applied in order to discard poorly reconstructed events.

4. Background rejection

Two sources of background have to be distinguished:

- (1) ϕ background:

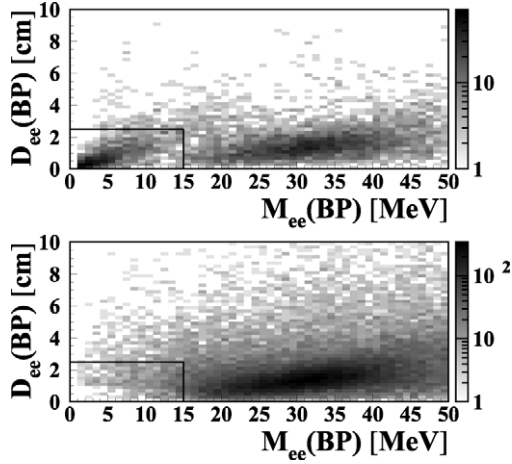


Fig. 1. D_{ee} vs M_{ee} evaluated at the beam pipe for ϕ background (top panel) and MC signal (bottom panel). Events in the box $M_{ee}(\text{BP}) < 15 \text{ MeV} \cap D_{ee}(\text{BP}) < 2.5 \text{ cm}$ are rejected.

this is mainly due to $\phi \rightarrow \pi^+\pi^-\pi^0$ events (with π^0 Dalitz decay) and to $\phi \rightarrow \eta\gamma$ events either with $\eta \rightarrow \pi^+\pi^-\pi^0$ (with π^0 Dalitz decay) or with $\eta \rightarrow \pi^+\pi^-\gamma$ (with photon conversion on the beam pipe). Note that this last background has the same signature as the signal. Background from $\phi \rightarrow K\bar{K}$ is also present at the preselection level.

(2) Continuum background:

this is due to $e^+e^- \rightarrow e^+e^-(\gamma)$ events with photon conversions, split tracks or interactions with some material in the region of DAΦNE quadrupoles inside KLOE. Because of poor MC statistics, this background has been studied using off-peak data taken at $\sqrt{s} = 1 \text{ GeV}$, where ϕ decays are negligible. This sample has been properly normalized for luminosity and \sqrt{s} behaviour.

A first background rejection is performed cutting on the sum of the absolute value of the momenta of the two particles having the highest momenta and opposite charge, $s2p = |\vec{p}(\text{p}_{\text{Max}}^+) + \vec{p}(\text{p}_{\text{Max}}^-)|$, and cutting on the sum of the absolute value of the momenta of the four selected tracks, $s4p = \sum_1^4 |\vec{p}_i|$. It is required that: ($270 < s2p < 460$) MeV and ($450 < s4p < 600$) MeV.

To reject the events due to photon conversion on the beam pipe, we extrapolate backward the e^+e^- candidate tracks, down to the intersection with the BP, and compute there the invariant mass (M_{ee}) and their distance (D_{ee}). A clear signal of photon conversion is visible in the $D_{ee}(\text{BP})$ – $M_{ee}(\text{BP})$ plane (Fig. 1). We reject events having $M_{ee}(\text{BP}) < 15 \text{ MeV}$ and $D_{ee}(\text{BP}) < 2.5 \text{ cm}$. The expected $M_{\pi\pi ee}$ spectrum before and after this cut is shown in Fig. 2. The ϕ background events peaked at the η invariant mass are significantly reduced by this cut.

Finally, to remove continuum background from interactions with quadrupoles, we have defined the quantities $\langle \cos\theta_f \rangle$ and $\langle \cos\theta_b \rangle$ as the average polar angle of forward and backward particles identified as signal. Events having $\langle \cos\theta_f \rangle > 0.85$ and $\langle \cos\theta_b \rangle < -0.85$ are rejected. This cut affects neither the signal nor background from ϕ decay events.

5. Fit to the $\pi^+\pi^-\pi^0 e^+e^-$ invariant mass spectrum and event counting

In order to evaluate the background contribution, we perform a fit to the data distribution of the $\pi^+\pi^-\pi^0 e^+e^-$ invariant mass after the cuts on the momenta. The fit is done on sidebands in order not to introduce correlations between signal and background. The ranges used are: $[450, 520] \text{ MeV} \cup [570, 650] \text{ MeV}$. Upper and

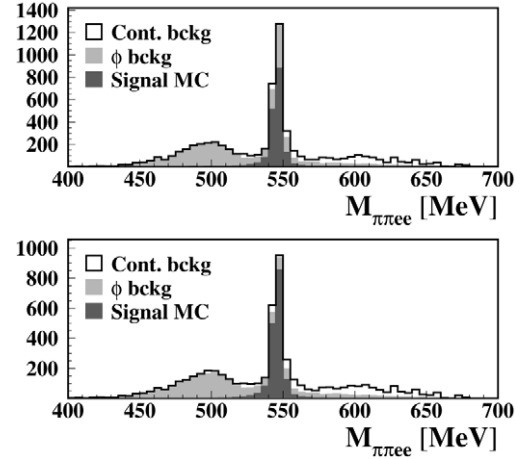


Fig. 2. Spectrum of the $\pi^+\pi^-\pi^0 e^+e^-$ invariant mass after the cuts on the momenta (top panel) and after the cut to reject events with photon conversions (bottom panel) have been applied. The black histogram is the expected distribution, i.e. signal MC (dark grey), ϕ background (light grey) and continuum background (white). The three samples have been normalized according to their luminosity.

Table 1

Event counting in the signal region.

Contribution	Counting
Data	1923.0
Signal	1555.0
Total background	368.0
ϕ background	275.2
Continuum background	92.8

lower limits (450 and 650 MeV) have been chosen in order not to include in the fit tails from background distributions. The central range (520 and 570 MeV) is wide enough to well contain the tails of the signal distribution. Then the fit is performed using the background shapes only.

The most precise background evaluation has been obtained fixing the off-peak data scale factor with luminosity at 7.14 ± 0.03 and fitting the MC background from ϕ meson decay. The output of the fit is $\chi^2/\text{dof} = 32.5/30$ ($P(\chi^2) = 0.35$), with a scale factor of 0.528 ± 0.009 , which is in good agreement with expectation from luminosity. The other possible approaches (fixing both the background scale factors with luminosity, leaving both free in the fit or fixing the ϕ decay and leaving free the continuum background shape) have been used for the evaluation of systematic uncertainties. The result of the fit is shown in Fig. 3 both in a wide $M_{\pi\pi ee}$ window and around the signal region.

For the signal estimate we limit ourselves to the region $[535, 555] \text{ MeV}$ and perform the event counting after background subtraction: we find 1555 (368) signal (background) events, see Table 1. Data-MC comparisons show a very good agreement for all considered variables. The most relevant distributions are reported in Fig. 4.

6. Measurement of the $BR(\eta \rightarrow \pi^+\pi^-\pi^0 e^+e^-(\gamma))$

The branching ratio has been evaluated according to the formula:

$$BR(\eta \rightarrow \pi^+\pi^-\pi^0 e^+e^-(\gamma)) = \frac{N_{\eta \rightarrow \pi^+\pi^-\pi^0 e^+e^-(\gamma)}}{N_{\eta\gamma}} \frac{1}{\epsilon_{\eta \rightarrow \pi^+\pi^-\pi^0 e^+e^-(\gamma)}}, \quad (1)$$

where $N_{\eta \rightarrow \pi^+\pi^-\pi^0 e^+e^-(\gamma)}$ is the number of signal events and $\epsilon_{\eta \rightarrow \pi^+\pi^-\pi^0 e^+e^-(\gamma)}$ is the efficiency taken from MC (the error accounts also for systematics on data-MC corrections). The number of $\phi \rightarrow \eta\gamma$ events, $N_{\eta\gamma}$, has been obtained using the formula

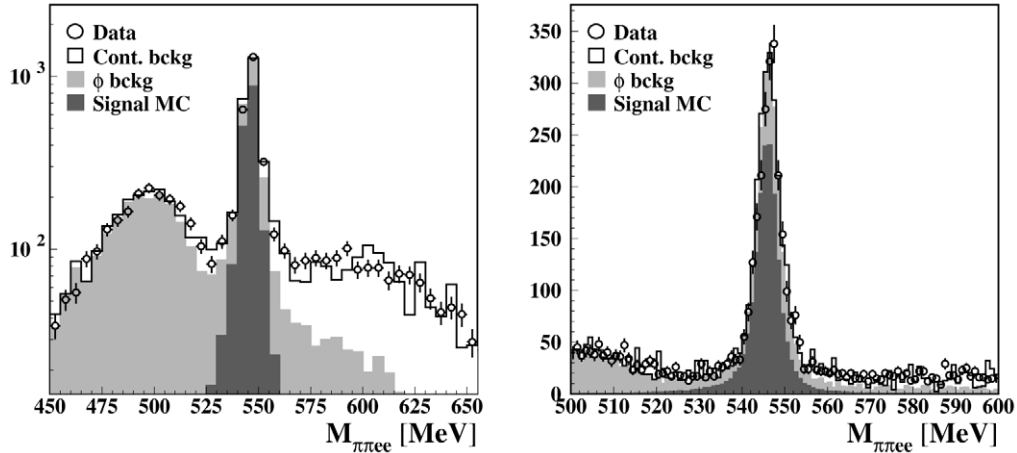


Fig. 3. $\pi^+\pi^-\pi^+e^-$ invariant mass spectrum on a wide range (left panel) and zoomed around the η mass (right panel). The background scale factors have been obtained as described in Section 5. Dots: data. The black histogram is the expected distribution, i.e. signal MC (dark grey), ϕ background (light grey) and continuum background (white).

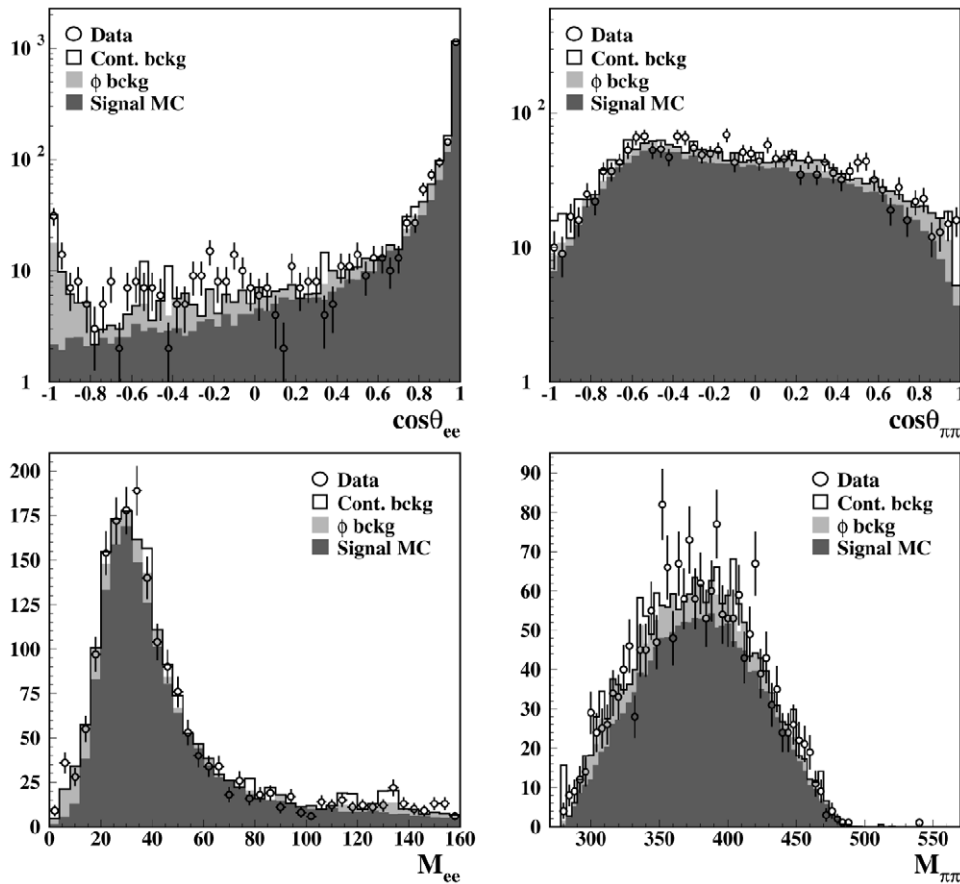


Fig. 4. Spectra of opening angle (top) and invariant mass (bottom) for the e^+e^- (left) and $\pi^+\pi^-$ (right) pairs for events in the signal region. The background scale factors have been obtained as described in Section 5. Dots: data. The black histogram is the expected distribution, i.e. signal MC (dark grey), ϕ background (light grey) and continuum background (white).

$N_{\eta\gamma} = \mathcal{L}\sigma_{\phi\rightarrow\eta\gamma}$, where \mathcal{L} is the integrated luminosity and the cross section $\sigma_{\phi\rightarrow\eta\gamma}$ takes into account the ϕ meson line shape. $\sigma_{\phi\rightarrow\eta\gamma}$ has been evaluated with $\eta \rightarrow \pi^0\pi^0\pi^0$ events collected in the range $1017 \text{ MeV} < \sqrt{s} < 1022 \text{ MeV}$ [26]. Inserting all the numbers summarized in Table 2, we obtain the value:

$$BR(\eta \rightarrow \pi^+\pi^-\pi^+e^+e^-(\gamma)) = (26.8 \pm 0.9_{\text{Stat.}}) \times 10^{-5}, \quad (2)$$

where the error accounts for the event counting and the background subtraction.

The systematic uncertainties have been evaluated in the following way:

- fixing with the luminosity or leaving free in the fit the background scale factors;
- varying the sideband upper and lower limits in the ranges [400, 535] MeV and [555, 700] MeV respectively;
- varying the binning of the histogram used for the fit from 1 MeV/bin to 5 MeV/bin;

Table 2

Summary of the numbers used in the master formula (1) for the branching ratio evaluation.

BR inputs	Values
Number of events	1555 ± 52
Efficiency	0.0803 ± 0.0004
Luminosity	$(1733 \pm 10) \text{ pb}^{-1}$
$e^+e^- \rightarrow \phi \rightarrow \eta\gamma$ cross section	$(41.7 \pm 0.6) \text{ nb}$

Table 3

Summary of the systematic uncertainties on the branching ratio.

Source of uncertainty	σ (BR)
Free/fixed scale factors	0.18×10^{-5}
Sidebands range	0.05×10^{-5}
Binning	0.02×10^{-5}
Analysis selection	0.55×10^{-5}
Normalization	0.42×10^{-5}
Total	0.72×10^{-5}

- repeating the whole analysis chain after moving selection criteria on $s2p$, $s4p$, D_{ee} (BP), M_{ee} (BP), $\langle \cos \theta_f \rangle$, $\langle \cos \theta_b \rangle$ and $M_{\pi\pi ee}$ by $\pm 1\sigma$, $\pm 2\sigma$'s, $\pm 3\sigma$'s around the reference value. The BR is then recomputed for all of these variations. The systematic uncertainty has been evaluated as the quadratic sum of RMS's obtained for each case.

The uncertainty on $N_{\eta\gamma}$ has been also added to the systematics in the normalization term. The results of the systematics evaluation are summarized in Table 3. The largest contributions are due to the normalization and to the cut on M_{ee} (BP). Taking the total systematic error into account, the measurement of the branching ratio is:

$$BR(\eta \rightarrow \pi^+\pi^-e^+e^-(\gamma)) = (26.8 \pm 0.9_{\text{Stat.}} \pm 0.7_{\text{Syst.}}) \times 10^{-5}. \quad (3)$$

7. Decay plane asymmetry evaluation

The decay plane asymmetry is calculated starting from the momenta of the four particles and is expressed as function of ϕ , the angle between the pion and the electron planes in the η rest frame (Fig. 5):

$$\mathcal{A}_\phi = \frac{N_{\sin\phi\cos\phi>0} - N_{\sin\phi\cos\phi<0}}{N_{\sin\phi\cos\phi>0} + N_{\sin\phi\cos\phi<0}}. \quad (4)$$

The quantity $\sin\phi\cos\phi$ is given by $(\hat{n}_{ee} \times \hat{n}_{\pi\pi}) \cdot \hat{z}(\hat{n}_{ee} \cdot \hat{n}_{\pi\pi})$, where the \hat{n} 's are the unit normals to the electron and pion planes and \hat{z} is the unit vector along the axis defined by the intersection of the two planes. The distribution of the $\sin\phi\cos\phi$ variable in the signal region is shown in Fig. 6. We remind that the signal MC has been produced with $\mathcal{A}_\phi = 0$.

While the analysis efficiency is completely flat in the $\sin\phi\cos\phi$ distribution, some distortion is introduced by the reconstruction, because of events with wrong mass assignment. The correction to this distortion has been evaluated by MC, fitting with a linear function the ratio between the generated and reconstructed $\sin\phi\cos\phi$ distributions. The resulting slope is -0.032 ± 0.016 . The use of higher polynomials does not improve the fit. The origin of this slope has been investigated by MC and it is completely due to the 14% of signal events with wrong particle identification. This because the particle identification algorithm forces the mass assignment in case of ambiguities without discarding events. The aim is to preserve the statistics, which completely dominates the asymmetry measurement.

The asymmetry has been evaluated for the events in the $535 \text{ MeV} < M_{\pi\pi ee} < 555 \text{ MeV}$ mass region after background sub-

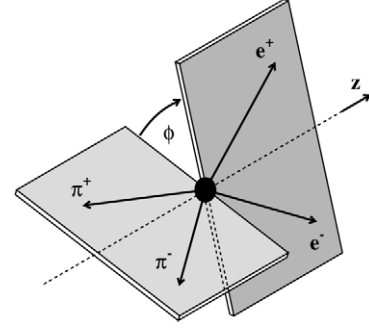


Fig. 5. Definition of the angle ϕ between the pion and electron decay planes.

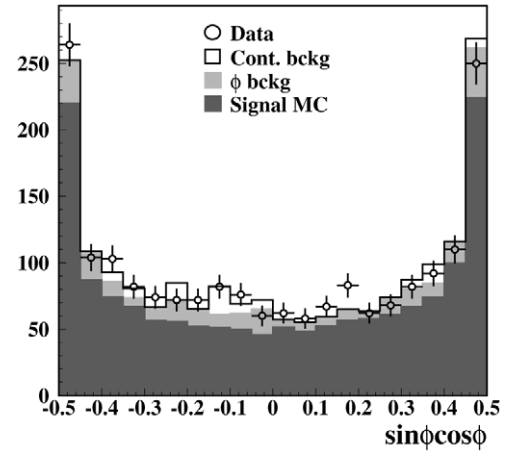


Fig. 6. Distribution of the $\sin\phi\cos\phi$ variable in the signal region. The background scale factors have been obtained as described in Section 5. Dots: data. The black histogram is the expected distribution, i.e. signal MC (dark grey), ϕ background (light grey) and continuum background (white).

traction. After applying the correction, we obtain:

$$\mathcal{A}_\phi = (-0.6 \pm 2.5_{\text{Stat.}} \pm 1.8_{\text{Syst.}}) \times 10^{-2}, \quad (5)$$

which is the first measurement of this asymmetry.

As for the branching ratio, the systematic error has been evaluated repeating the whole analysis chain after varying selection criteria by $\pm 1\sigma$, $\pm 2\sigma$'s and $\pm 3\sigma$'s around the reference value and taking as uncertainty the quadratic sum of the resulting RMS's. The uncertainty due to the correction has been evaluated varying its slope by $\pm 1\sigma$. The largest contribution is due to the cut on $M_{\pi\pi ee}$ while the contribution of the slope correction is 0.5×10^{-2} .

In order to check the distortion correction applied to \mathcal{A}_ϕ , we have defined a control sample having only events without ambiguities in particle identification. In this case the probability of wrong particle identification is almost zero and no distortions are observed in the MC $\sin\phi\cos\phi$ distribution. The fraction of this control sample in data and MC events is in good agreement (0.62 ± 0.02 and 0.64 ± 0.02 respectively), showing that our simulation reproduces the real data well. The asymmetry evaluated with the control sample is in good agreement with our measurement but has a larger statistical error: $\mathcal{A}_\phi = (-1.2 \pm 3.1_{\text{Stat.}}) \times 10^{-2}$.

8. Conclusions

Using a sample of 1.7 pb^{-1} collected in the ϕ meson mass region, we have obtained a measurement of the $\eta \rightarrow \pi^+\pi^-e^+e^-(\gamma)$ branching ratio with 4% accuracy, ten times more precise than the previous best measurement [6–8]:

$$BR(\eta \rightarrow \pi^+\pi^-e^+e^-(\gamma)) = (26.8 \pm 0.9_{\text{Stat.}} \pm 0.7_{\text{Syst.}}) \times 10^{-5}. \quad (6)$$

Radiative events slightly modify momentum distribution of the charged particles and have been carefully considered in the efficiency evaluation. As a result, the measured branching ratio is fully radiation inclusive.

Our measurement is about 2σ smaller than theoretical predictions [3–5], while it is in agreement ($\sim 1\sigma$) with the calculations of the ratio of the branching fractions $BR(\eta \rightarrow \pi^+\pi^-e^+e^-)/BR(\eta \rightarrow \pi^+\pi^-\gamma)$ in references [2,5] when the recent CLEO measurement of $BR(\eta \rightarrow \pi^+\pi^-\gamma)$ [27] is used as normalization.

The final sample of 1555 signal events allows us to perform the first measurement of the CP-violating asymmetry \mathcal{A}_ϕ , which is consistent with zero at the 3% percent precision level:

$$\mathcal{A}_\phi = (-0.6 \pm 2.5_{\text{Stat.}} \pm 1.8_{\text{Syst.}}) \times 10^{-2}. \quad (7)$$

Acknowledgements

We would like to thank D.N. Gao for the useful discussions. We thank the DAΦNE team for their efforts in maintaining low background running conditions and their collaboration during all data-taking. We want to thank our technical staff: G.F. Fortugno and F. Sborzacchi for their dedicated work to ensure an efficient operation of the KLOE Computing Center; M. Anelli for his continuous support to the gas system and the safety of the detector; A. Balla, M. Gatta, G. Corradi and G. Papalino for the maintenance of the electronics; M. Santoni, G. Paoluzzi and R. Rosellini for the general support to the detector; C. Piscitelli for his help during major maintenance periods. This work was supported in part by EURODAHNE, contract FMRX-CT98-0169; by the German Federal Ministry of Education and Research (BMBF) contract 06-KA-957; by the German Research Foundation (DFG), ‘Emmy Noether Programme’, contracts DE839/1–4; and by the EU Integrated Infrastructure

Initiative HadronPhysics Project under contract number RII3-CT-2004-506078.

References

- [1] L.G. Landsberg, Phys. Rep. 128 (1985) 301.
- [2] C. Jarlskog, H. Pilkuhn, Nucl. Phys. B 1 (1967) 264.
- [3] A. Faessler, C. Fuchs, M.I. Krivoruchenko, Phys. Rev. C 61 (2000) 035206.
- [4] C. Picciotto, S. Richardson, Phys. Rev. D 48 (1993) 3395.
- [5] B. Borasoy, R. Nissler, Eur. Phys. J. A 33 (2007) 95.
- [6] R.R. Akhmetshin, et al., CMD-2 Collaboration, Phys. Lett. B 501 (2001) 191.
- [7] C. Bargholtz, et al., CELSIUS-WASA Collaboration, Phys. Lett. B 644 (2007) 299.
- [8] C. Berlowski, et al., Phys. Rev. D 77 (2008) 032004.
- [9] L.M. Sehgal, M. Wanninger, Phys. Rev. D 46 (1992) 1035; L.M. Sehgal, M. Wanninger, Phys. Rev. D 46 (1992) 5209, Erratum.
- [10] P. Heiliger, L.M. Sehgal, Phys. Rev. D 48 (1993) 4146; P. Heiliger, L.M. Sehgal, Phys. Rev. D 60 (1999) 079902, Erratum.
- [11] J.K. Elwood, M.B. Wise, M.J. Savage, Phys. Rev. D 52 (1995) 5095; J.K. Elwood, M.B. Wise, M.J. Savage, Phys. Rev. D 53 (1996) 2855, Erratum.
- [12] J.K. Elwood, M.B. Wise, M.J. Savage, J.W. Walden, Phys. Rev. D 53 (1996) 4078.
- [13] G. Ecker, H. Pichl, Phys. Lett. B 507 (2001) 193.
- [14] A. Alavi-Harati, et al., KTeV Collaboration, Phys. Rev. Lett. 84 (2000) 408.
- [15] A. Lai, et al., NA48 Collaboration, Phys. Lett. B 496 (2000) 137.
- [16] F. Ambrosino, et al., KLOE Collaboration, Phys. Lett. B 606 (2005) 276.
- [17] C. Jarlskog, E. Shabalin, Phys. Rev. D 52 (1995) 248.
- [18] C.Q. Geng, J.N. Ng, T.H. Wu, Mod. Phys. Lett. A 17 (2002) 1489.
- [19] D.N. Gao, Mod. Phys. Lett. A 17 (2002) 1583.
- [20] M. Adinolfi, et al., KLOE Collaboration, Nucl. Instrum. Methods A 488 (2002) 51.
- [21] M. Adinolfi, et al., KLOE Collaboration, Nucl. Instrum. Methods A 482 (2002) 364.
- [22] M. Adinolfi, et al., KLOE Collaboration, Nucl. Instrum. Methods A 492 (2002) 134.
- [23] F. Ambrosino, et al., KLOE Collaboration, Nucl. Instrum. Methods A 534 (2004) 403.
- [24] E. Barberio, Z. Was, Comput. Phys. Commun. 79 (1994) 291.
- [25] P. Golonka, Z. Was, Eur. Phys. J. C 45 (2006) 97.
- [26] S. Giovannella, S. Miscetti, KLOE note 212, 2006, <http://www.lnf.infn.it/kloe/pub/knote/kn212.ps>.
- [27] A. Lopez, et al., CLEO Collaboration, Phys. Rev. Lett. 99 (2007) 122001.